Femtosecond Phase-and-Polarization Control for Background-Free Coherent Anti-Stokes Raman Spectroscopy

Dan Oron, Nirit Dudovich, and Yaron Silberberg

Department of Physics of Complex Systems, Weizmann Institute of Science, Rehovot 76100, Israel

(Received 2 December 2002; published 30 May 2003)

Phase-and-polarization coherent control is applied to control the nonlinear response of a quantum system. We use it to obtain high-resolution background-free single-pulse coherent anti-Stokes Raman spectra. The ability to control both the spectral phase and the spectral polarization enables measurement of a specific off-diagonal susceptibility tensor element while exploiting the different spectral response of the resonant Raman signal and the nonresonant background to achieve maximal background suppression.

DOI: 10.1103/PhysRevLett.90.213902 PACS numbers: 42.65.Dr, 32.80.Qk, 78.47.+p

The goal of coherent control is to steer a quantum system towards a desirable outcome, by inducing constructive interference between paths leading to it, while inducing destructive interference between paths leading to other outcomes. Shaping of the spectral phase of the incoming pulses has been the main tool of this rapidly growing field. Among numerous applications, phase-shaped pulses have been used to control multiphoton absorption [1], branching ratios of chemical reactions [2], and high-harmonic generation [3]. Recently, Brixner *et al.* [4] have shown that by some modification of the conventional phase-only pulse shaper, the spectral polarization of an ultrashort pulse can be controlled as well. These extra degrees of freedom enable us to greatly improve the controllability of the quantum system. We report here how the control of both the spectral phase and the spectral polarization enables us to obtain background-free single-pulse coherent anti-Stokes Raman (CARS) spectra with a high spectral resolution.

CARS is a four-wave mixing process involving the generation of a coherent vibration in the probed medium [5]. In CARS, a pump photon ω_p, a Stokes photon ω_s, and a probe photon ω_{pr} mix to emit a signal photon $\omega_p - \omega_s + \omega_{pr}$. The energy level diagram of this process is schematically plotted in Fig. 1(a). Resonant enhancement occurs when the energy difference $\omega_p - \omega_s$ coincides with a vibrational level of the medium. Typically, two narrow band sources at ω_p and at ω_s are used to generate a signal at $2\omega_p - \omega_s$ (in this case, $\omega_{pr} = \omega_p$). The use of a narrow band probe and a broad band Stokes beam has enabled simultaneous measurement of an entire band of the Raman spectrum (multiplex CARS) [5]. Coherent Raman processes have become a valuable tool in femtosecond time-resolved spectroscopy, combustion studies, and condensed-state spectroscopy. CARS has recently become a favorable method for multiphoton depth-resolved microscopy [6,7].

Another possibility to obtain multiplex CARS spectra is by impulsive excitation of the Raman level with a broad band pulse, followed by probing with a narrow band probe pulse. The typically weak signal can be separated either spectrally (as in pump-probe experiments) or spatially (as in transient grating experiments). This sort of scheme suffers from an increased spectrally broad nonresonant background due to the impulsive excitation. Moreover, the experimental setup, either in the pump-probe approach, or in the transient grating approach is cumbersome. This approach has, therefore, not been pursued in recent years.

In a new approach, single-pulse CARS spectroscopy with phase-controlled ultrashort pulses, of a duration of the order of 20 fs, has been presented [8]. This spectroscopy method relied on the selective excitation of Raman levels with a spectral resolution of about 30 cm^{-1}, nearly 2 orders of magnitude better than the pulse bandwidth. Single-pulse multiplex CARS has recently been presented [9]. In this scheme, a narrow spectral band in the excitation pulse is phase shifted, serving as an effective probe, and the Raman spectrum is extracted from the interference pattern of the resonant signal with the nonresonant background. The main advantage of the single-pulse CARS approach is its simplicity: it requires only a single fixed-frequency ultrafast laser source, rather than synchronized tunable sources as in standard multicolor CARS. The most significant issue in single-pulse CARS using phase-controlled pulses is dealing with the relatively strong nonresonant background without loss of

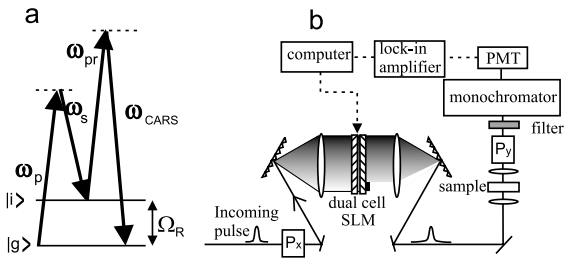

FIG. 1. (a) Energy level diagram of the CARS process. (b) Outline of the experimental setup: P_x, P_y are polarizers for *x, y* polarizations, respectively.

spectral information. Since phase control only implies changes in the temporal profile of the pulse, this background cannot be reduced to values below those observed in standard two-color picosecond CARS, where the duration of the pulse matches the Raman level decoherence time. This is in contrast to polarization techniques in two-color CARS which reduce the nonresonant background to significantly lower values by measuring a nonlinear susceptibility component such as $|\chi_{yxyx} - \chi_{yyxx}|^2$ which, due to the Kleinmann symmetry [10], vanishes for nonresonant transitions [11].

The newly suggested technique of femtosecond phase and polarization pulse shaping [4] enables the incorporation of polarization techniques in single-pulse CARS. In this technique, the spatial light modulator acts as both a controlled spectral phase mask and as a spectrally variable wave plate at an angle of 45°. In the following we demonstrate first how polarization control can be used to break the ultrashort pulse into a broad band pump and a narrow band probe with orthogonal polarizations for multiplex CARS. This naive approach, however, yields rather poor results due to the strong nonresonant background. We then show how the combination of both phase and polarization control can lead to nearly complete suppression of the nonresonant term, yielding background-free single-pulse multiplex CARS spectra with a high spectral resolution.

The nonlinear polarization producing the CARS signal driven by an electric field whose complex spectral amplitude is $\epsilon(\omega)$ can be approximated for nonresonant transitions [12]:

$$P_j^{(3)}(\omega) \propto \chi_{jklm}^{nr} \int_0^\infty d\Omega \epsilon_k(\omega - \Omega) A_{lm}(\Omega), \qquad (1)$$

where $A_{lm}(\Omega) = \int_0^\infty d\omega \epsilon_l^*(\omega - \Omega)\epsilon_m(\omega)$ is the second order polarization driving molecular vibrations, and $jklm$ denote the electric field polarizations. For a singly resonant Raman transition through an intermediate level $|i\rangle$ at an energy of $\hbar \cdot \Omega_R$ and a bandwidth Γ we obtain

$$P_j^{(3)}(\omega) \propto \chi_{jklm}^{r} \int_0^\infty d\Omega \frac{\epsilon_k(\omega - \Omega)}{(\Omega_R - \Omega) + i\Gamma} A_{lm}(\Omega). \qquad (2)$$

The two main differences between the resonant and nonresonant components are the following: first, the resonant component has a narrow spectral response, centered at $\Omega = \Omega_R$, whereas the spectral response of the nonresonant component is broad. Second, the response of the resonant component inverts sign about $\Omega = \Omega_R$ while the nonresonant response has a constant phase. In the following, we show how these differences are used to reduce one while enhancing the other.

To demonstrate single-pulse polarization CARS spectroscopy, we considered Raman transitions in several simple molecules. The impulsive excitation is driven by 20 fs full-width at half maximum (FWHM) transform-limited pulses, centered at 815 nm (corresponding to a bandwidth of about 70 nm), generated by a Ti:sapphire laser oscillator operating at 80 MHz. The pulse energy was about 0.5 nJ. Spectral phases and polarizations were applied by a programmable pulse shaper, which includes two liquid crystal spatial light modulator (SLM) arrays whose preferential orientation axes are at right angles to each other [4,13], and are rotated by $\pm 45°$ relative to the polarization of the input beam. Any difference in the applied retardance between the two arrays results in modification of the input beam polarization. An additional retardance applied to both arrays results in modification of the spectral phase [14]. The spectral resolution, determined by the spot size at the Fourier plane, is about 0.3 nm (equivalent to about 5 cm^{-1}). Each pixel on the SLM covers about 9 cm^{-1}. Wavelengths shorter than 780 nm are blocked at the Fourier plane as they spectrally overlap the CARS signal. A spectral band between 780 and 855 nm (corresponding to an energy span of 1100 cm^{-1}) was used to induce the CARS process. The shaped pulse was focused into the sample using a $NA = 0.2$ objective. The CARS signal was filtered by both a sharp-cut short pass filter at 766 nm (Omega optical), and a computer-controlled monochromator with a spectral resolution of 0.5 nm and measured with a photomultiplier tube (PMT) and a lock-in amplifier. An outline of the experimental setup is shown in Fig. 1(b). The measurable Raman energy range of our system is about 300–900 cm^{-1}. The lower limit is determined by the need to filter out the excitation pulse. The upper limit is dictated by the excitation pulse bandwidth.

The simplest approach to single-pulse polarization controlled CARS would be to rotate the polarization of the excitation pulse in a narrow band at its high-energy end, from the x plane to the y plane [as shown schematically in Figs. 2(a) and 2(b)], and monitor the CARS signal in the y plane. When this is done, the monitored signal is effectively dependent only on A_{xx} as the driving polarization field, and on ϵ_y as a probe. Since ϵ_y is spectrally narrow, the resonant term generates a narrow band feature, whose width is the convolution of the probe bandwidth and the Raman level linewidth, in the CARS signal spectrum. This is in contrast with the nonresonant term which results in a broad band background, due to the broad band excitation.

We note that in addition to contributions from χ_{yyxx}, where the y-polarized band acts as probe, there are also contributions from χ_{yxxy}, where it acts as pump. The resonant term is, however, dominated by the isotropic χ_{yyxx}^r contribution, since A_{xx} is a broad band impulsive excitation, leading to a significantly larger Raman level population than A_{xy} which is a narrow band one. The ratio between the two increases as the probe bandwidth is decreased and is typically larger than 1 order of magnitude. Moreover, the A_{xy} contribution is further reduced for vibrations with low depolarization ratios [15]. For the

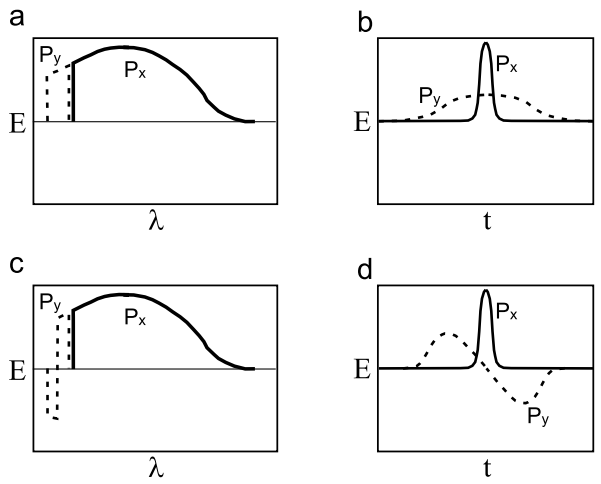

FIG. 2. Schematic drawings of the spectral (a),(c) and temporal (b),(d) electric field amplitudes in both the x polarization (solid line) and the y polarization (dashed line) for excitation pulses used in our experiments: polarization-only shaped pulses (a),(b) and phase and polarization shaped pulses (c),(d). A shift of the spectral phase by π [in (c)] is equivalent to a sign inversion of the electric field amplitude in a band within the y-polarized component. For convenience, the temporal field amplitudes (b),(d) have been normalized. In practice, the peak field amplitude of the x-polarized component is an order of magnitude higher than that of the y component.

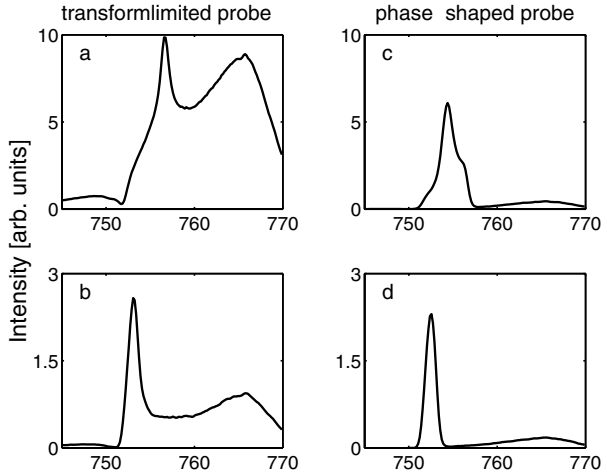

FIG. 3. Measured CARS spectra from a iodomethane sample (resonant at 523 cm^{-1}. The spectra on the left column (a),(b) were obtained with polarization-only shaping. The spectra on the right column (c),(d) were obtained with a π phase step applied in the central frequency of the probe. The total bandwidth of the probe decreases from top to bottom: 4.5 nm (a),(c); 1.2 nm (b),(d).

nonresonant signal $\chi^{nr}_{yyxx} = \chi^{nr}_{yxxy}$ (Kleinmann symmetry), so both contributions are equal in magnitude and indistinguishable. The total nonresonant contribution to the CARS signal is thus a replica of that induced by the χ^{nr}_{yyxx} term alone.

As in multicolor CARS, the ratio of the resonant signal to the nonresonant background, as well as the spectral resolution, improves as the probe pulse becomes longer. In our case, the duration of the probe pulse is determined by the spectral width of the polarization shifted band. The dependence of both the resonant and nonresonant terms on the probe spectral width is demonstrated in Figs. 3(a) and 3(b), where the CARS spectrum from liquid iodomethane is plotted for two probe bandwidths. As the probe bandwidth is decreased from about 4.5 nm [corresponding to 400 fs, see Fig. 3(a)] to about 1.2 nm [corresponding to 1.5 ps, see Fig. 3(b)] the resonant signal, due to its narrow spectral response, becomes narrower but maintains its strength. In contrast, the nonresonant background, having a broad spectral response, becomes weaker but maintains its spectral shape. Since the two are coherent, they generate an interference pattern, interfering constructively at the low-energy end of the probe pulse, and destructively at its high-energy end. This interference pattern obscures the interpretation, making it difficult to extract either the strength or the exact spectral location of the resonant peak, and calls for further reduction of the nonresonant background.

Reduction of the nonresonant background can be achieved by using the second available degree of freedom—phase control. We introduce a π phase step at the center of the polarization shifted band serving as probe [as shown in Fig. 2(c)]. We thus split our probe to two spectrally distinct longer probe pulses with opposite phase. Because of the broad nonresonant spectral response, the nonresonant background from these two probe pulses interferes destructively. Since $A_{xx}(\Omega)$ is a very smooth function, the two are almost equal in magnitude. As a result, the nonresonant background can be reduced by orders of magnitude. This reduction can be alternatively viewed in the time domain. The π phase step modifies the temporal shape of the y-polarized probe so that the electric field envelope crosses zero at the peak of the x-polarized driving field, as can be seen in Fig. 2(d). Because of the instantaneous nonresonant response, the nonresonant background is almost completely suppressed. The resonant signal response is different. The π phase step compensates for the sign inversion of the denominator in Eq. (2), leading to an increased resonant signal over a narrow spectral band shifted by the Raman level energy from the π step location, as has been demonstrated in Ref. [12]. CARS spectra with a phase-shaped probe pulse are presented in Figs. 3(c) and 3(d), where the total probe bandwidth is, again, either 4.5 nm [Fig. 3(c)] or 1.2 nm [Fig. 3(d)]. Comparing the measured spectra with transform-limited vs phase-shaped probe pulses, a dramatic decrease in the nonresonant background is seen. The small nonresonant background still observed using the phase-shaped probe is in fact a small fraction ($\approx 0.05\%$) of the χ_{xxxx} component which "leaks" through the polarizer due

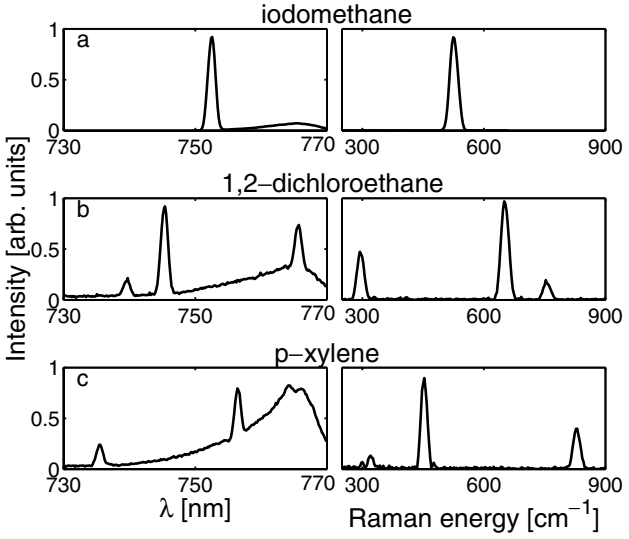

FIG. 4. Normalized measured CARS spectra (left column) and the extracted Raman spectra after background subtraction (right column) from: (a) iodomethane (resonant at 523 cm^{-1}). (b) 1,2-dichloroethane (resonant at 298, 652, and 750 cm^{-1}). (c) *p* xylene (resonant at 313, 459, and 830 cm^{-1}).

to small birefringence of the microscope objective and collection optics. This background term is independent of the applied phase and polarization and can be easily subtracted. In Fig. 3(c) the resonant signal can be seen to have a spectral shape of a broader pedestal on top of which lies a sharp peak, as observed in Ref. [12]. This shape is slightly distorted by the weak nonresonant background. The spectral resolution of the sharp peak is better than 20 cm^{-1}. We find, however, that even with a phase-shaped probe it is better to work with a narrower bandwidth.

In Fig. 4 we present Raman spectra of several simple molecules, all in the liquid phase, as measured with phase and polarization shaped pulses, where the total probe bandwidth was 1.2 nm, including a π step at its center. The measured CARS spectra are plotted on the left column, and the extracted Raman spectra, from which the background due to birefringence was subtracted are plotted on the right column. Figure 4(a) shows the 523 cm^{-1} Raman level of iodomethane. The FWHM of this peak is about 15 cm^{-1}. The measured Raman spectrum of 1,2-dichloroethane is plotted in Fig. 4(b). The 652 cm^{-1} and the 750 cm^{-1} levels, separated by 98 cm^{-1}, are seen as two very well separated peaks. The 298 cm^{-1} level is at the lower limit of the detectable region. The Raman spectrum of *p* xylene, with a level at 830 cm^{-1}, as shown in Fig. 4(c), demonstrates the ability to observe the high-energy end of the detectible region.

In this Letter we have shown how simultaneous phase-and-polarization shaping leads to single-pulse measurement of a resonant off-diagonal component of a CARS four-wave mixing process with very good nonresonant background rejection (which can be further improved with properly chosen reduced birefringence optical components). Using slightly shorter pulses, available in commercial systems today, this measurement technique can yield Raman spectra spanning the entire fingerprint region (up to 1500 cm^{-1}) [16]. Phase-and-polarization shaping enables the crafting of two independently shaped, orthogonal polarization pulses that are used as the excitation and probe pulses for the CARS process. This form of single-pulse Raman spectroscopy is a demonstration of the capabilities and promise of this new pulse shaping technique. We believe this method will have a considerable impact both on nonlinear spectroscopy and on the field of molecular coherent control.

The authors would like to thank Dr. Tobias Brixner and Professor Gustav Gerber for helpful and stimulating discussions on their polarization shaping technique. Financial support of this research by the Israel Science Foundation and by the German BMBF is gratefully acknowledged.

[1] D. Meshulach and Y. Silberberg, Nature (London) **396**, 239 (1998).
[2] A. Assion *et al.*, Science **282**, 919 (1998).
[3] R. Bartels *et al.*, Nature (London) **406**, 164 (2000).
[4] T. Brixner and G. Gerber, Opt. Lett. **26**, 557 (2001); T. Brixner, G. Krampert, P. Niklaus, and G. Gerber, Appl. Phys. B **74**, S133 (2002).
[5] *Infrared and Raman Spectroscopy*, edited by B. Schrader (VCH, Weinheim, 1995).
[6] A. Zumbusch, G. R. Holtom, and X. S. Xie, Phys. Rev. Lett. **82**, 4142 (1999).
[7] M. Muller and J. M. Schins, J. Phys. Chem. B **106**, 3715 (2002).
[8] N. Dudovich, D. Oron, and Y. Silberberg, Nature (London) **418**, 512 (2002).
[9] D. Oron, N. Dudovich, and Y. Silberberg, Phys. Rev. Lett. **89**, 273001 (2002).
[10] R.W. Boyd, *Nonlinear Optics* (Academic Press, San Diego, 1992).
[11] J. J. Song, G. L. Eesley, and M. D. Levenson, Appl. Phys. Lett. **29**, 567 (1976).
[12] D. Oron, N. Dudovich, D. Yelin, and Y. Silberberg, Phys. Rev. Lett. **88**, 063004 (2002).
[13] M. M. Wefers and K. A. Nelson, Opt. Lett. **18**, 2032 (1993).
[14] Note that our phase and polarization scheme utilizes only linear polarizations oriented along either the *x* or the *y* axis. Moreover, it is insensitive to the relative phase between the two polarization axes. We thus circumvent several problems associated with the sensitivity of optical components to the polarization orientation, as discussed in Ref. [4].
[15] W. Li, H.-G. Purucker, and A. Laubereau, Opt. Commun. **94**, 300 (1992); Y. Saito, T. Ishibashi, and H. Hamaguchi, J. Raman Spectrosc. **31**, 725 (2000).
[16] N. Dudovich, D. Oron, and Y. Silberberg, J. Chem. Phys. **118**, 9208 (2003).